

ChemComm

Accepted Manuscript



This is an *Accepted Manuscript*, which has been through the Royal Society of Chemistry peer review process and has been accepted for publication.

Accepted Manuscripts are published online shortly after acceptance, before technical editing, formatting and proof reading. Using this free service, authors can make their results available to the community, in citable form, before we publish the edited article. We will replace this *Accepted Manuscript* with the edited and formatted *Advance Article* as soon as it is available.

You can find more information about *Accepted Manuscripts* in the [Information for Authors](#).

Please note that technical editing may introduce minor changes to the text and/or graphics, which may alter content. The journal's standard [Terms & Conditions](#) and the [Ethical guidelines](#) still apply. In no event shall the Royal Society of Chemistry be held responsible for any errors or omissions in this *Accepted Manuscript* or any consequences arising from the use of any information it contains.

COMMUNICATION

Cytosine-bulge-dependent fluorescence quenching for real-time hairpin primer PCR

F. Takei, X. Chen, G. Yu, T. Shibata, C. Dohno and K. Nakatani*

Cite this: DOI: 10.1039/x0xx00000x

Received 00th January 2012,
Accepted 00th January 2012

DOI: 10.1039/x0xx00000x

www.rsc.org/

The progress of polymerase chain reaction (PCR) was sensitively monitored based on the increase in fluorescence of *N,N'*-bis(3-aminopropyl)-2,7-diamino-1,8-naphthyridine, which was covalently anchored on the cytosine bulge directly neighbouring the 5'-T_G-3'/5'-CCA-3' sequence in the hairpin tag at the 5' end of PCR primer.

Recent progress in the labelling chemistry of oligonucleotides has provided many types of fluorogenic probes.¹⁻¹⁷ Fluorogenic hybridization probes were designed to report the hybridization state with the target nucleic acids according to the change in fluorescent properties; e.g., wavelength, intensity, lifetime, and so on.¹⁸⁻²¹ These probes are useful for analysing single nucleotide polymorphisms (SNPs),²²⁻²⁴ for detecting and imaging RNA both *in vitro* and *in vivo*,²⁵ and for monitoring biological reactions.²¹ TaqMan[®] probe,²⁶ one of hybridization probes labelled with a fluorophore and its quencher, has been used to monitor the real-time progress of a polymerase chain reaction (PCR).²⁷ PCR is one of the most fundamental technologies in molecular biology studies and enables the quantitative determination of the amount of nucleic acids in a sample and to identify SNPs by allele-specific PCR.²⁸⁻³⁰ While TaqMan[®] probe is a *de facto* standard probe for quantitative PCR, further innovation in the real-time monitoring of PCR progress is still needed to simplify the PCR experiments and to evade the time- and cost-consuming probe synthesis. Toward this end, we anticipated that the function of reporting the PCR progress could be integrated into the PCR primers themselves.

The major challenge involved in monitoring PCR progress using fluorescently labelled primers is to translate the PCR progress into any changes occurring in the properties of fluorescent chromophores. We have addressed this issue by exploiting the concept of secondary structure-inducible fluorescence change.³¹⁻³³ Thus, we coupled the structural change on a hairpin DNA tag attached at the 5' end of the primer with the fluorescence emission of a ligand selectively bound to the hairpin form. The ligand binds to the cytosine bulge (C-bulge) embedded in the hairpin tag that will be opened and transformed into

double-stranded form by PCR. This hairpin primer PCR is successful in monitoring PCR progress in real-time and can be used for SNP typing by allele-specific PCR,³⁴ as well as for virus detection.^{35,36} One drawback of the hairpin primer PCR, however, is that the fluorescent signal decreases with progression of the PCR cycle. Detection of a signal increasing from a low background level is more advantageous than detection of a signal decreasing from a high background level with regard to the sensitivity and detection range. We here report our attempt to improve the hairpin primer PCR from detection of a decreasing signal to one of an increasing signal.

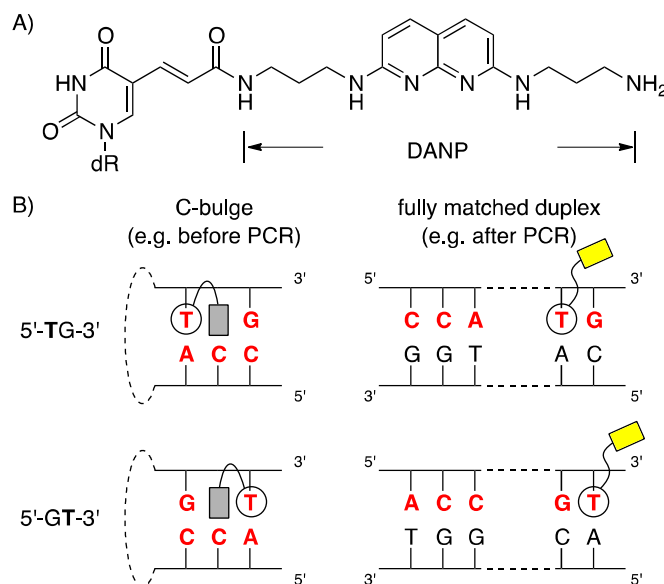


Fig. 1 A) Structure of DANP anchored at the C5 of thymine. B) Illustration of a proposed structure-fluorescence matrix of DANP covalently anchored at the hairpin tag in two possible (top) 5'-TG-3' and (bottom) 5'-GT-3' sequences and in (left) C-bulge form (i.e., before PCR) and (right) duplex form (i.e., after PCR). Grey

rectangles indicate the DANP with quenched fluorescence, whereas yellow rectangles show the DANP emitting fluorescence. Dotted lines represent a hairpin loop in the case of the hairpin primer.

In hairpin primer PCR, *N,N'*-bis(3-aminopropyl)-2,7-diamino-1,8-naphthyridine (DANP) binds to the C-bulge in the hairpin tag and is released from the C-bulge upon hairpin opening by the polymerase reaction. DANP emits fluorescence at 400–450 nm upon binding to the C-bulge,^{37,38} and the emission spectra are sensitively modulated by the base pairs flanking the C-bulge. The A-T base pairs directly neighbouring the C-bulge induce the emission shift toward a longer wavelength by approximately 30 nm, whereas the G-C flanking base pairs quench the DANP fluorescence. The affinity of DANP binding to the C-bulge flanking A-T base pairs was about 1 μM (K_d), and affinity to the fully complementary double-stranded DNA was very weak. With these observations in mind, we hypothesized that the fluorescence of DANP anchored close to the C-bulge flanking the G-C base pair would be effectively quenched when DANP bound to the C-bulge, but not when DANP was released from the C-bulge□□□□□dangling on the□□□□□□□□□□the □□□□□□ (Fig. 1)□ Accordingly, the increase of DANP fluorescence could be observed upon structural changes induced by the polymerase reaction from the hairpin form holding the C-bulge to a fully complementary double-stranded form.

First, we investigated the sequence of the C-bulge and the manner of DANP anchoring. The DANP-anchored probe must have at least one G-C base pair at the flanking site of the DANP-binding C-bulge to effectively quench the DANP fluorescence. To anchor DANP at the methyl group of the thymine, we selected an A-T base pair for the other flanking base pair to yield two possible sequences 5'-*T*_G-3'/3'-ACC-5' and 5'-G_*T*-3'/3'-CCA-5', where *T* is the site of DANP anchoring (Fig. 1B). For the facile anchoring of DANP onto the thymine next to the C-bulge site, the reaction of *N*-hydroxysuccinimide ester of (2'-deoxyuridin-5-yl)acrylic acid on the DNA intermediate growing on the support of the controlled pore glass (CPG) with the primary amine of DANP was designed. Molecular modelling simulations (Maestro ver. 9.7, Schrödinger) suggested that DANP anchored at the T in both the 5'-*T*_G-3'/3'-ACC-5' and 5'-G_*T*-3'/3'-CCA-5' sequences would be suitable for the binding of DANP to the neighbouring C-bulge. The synthetic procedure for DNAs containing DANP-anchored thymine is described in Scheme S1. In brief, the CPG-attached DNA precursor containing *N*-hydroxysuccinimide ester of (2'-deoxyuridin-5-yl)acrylic acid was synthesized using the standard phosphoramidite method and supplied by Japan Bio Services (Saitama, Japan). The activated ester was reacted with 0.1 \square M DANP in dimethyl sulfoxide (DMSO) and incubated at 37 \square C for approximately 3 hours. After the filtration of excess DANP and DMSO, the DANP-anchored DNA was cleaved from the CPG, deprotected by an ammonia solution at room temperature, and purified by reverse-phase high-performance liquid chromatography.

We then investigated the thermodynamic properties, absorption spectra, and fluorescence spectra of the DANP-anchored DNA. The melting temperature (T_m) of the duplex (**M1/3**) consisting of DANP-anchored DNA **M1** 5'-TCCAT_GCAAC-3' (5'-T_G-3') and the C-bulge strand **3** 5'-GTTGCCATGGA-3' (5'-CCA-3') was 41.5 °C, which was 14.4 °C higher than that of the unmodified C-bulge duplex (**U1/3**, T_m 27.1 °C) (Table 1; complete sequences of the oligonucleotides used in these studies are shown in the Supporting information, Table S1). In contrast, the T_m of the duplex **M2/5** consisting of the DANP-anchored DNA **M2** 5'-TCCAG_TCAAC-3' (5'-G_T-3') and the C-bulge strand **5** 5'-GTTGACCTGGA-3' (5'-ACC-3') was only 1.2 °C higher than that

of unmodified duplex (**U2/5**). Anchoring DANP to the T was found to weakly destabilize the fully matched duplex, as is seen by the T_m difference between **M1/4** and **U1/4** (-2.4 °C), and **M2/6** and **U2/6** (-0.4 °C), emphasizing a large increase in the thermodynamic stability of the C-bulge duplex due to DANP anchoring at the neighbouring T.

Table 1. Melting temperatures of the DANP-anchored C-bulge and duplex.

Sequence	T_m °C	Sequence	T_m °C
M1/3: 5'- T G-3' 3'-ACC-5'	41.5	M2/5: 5'-G T -3' 3'-CCA-5'	28.5
U1/3: 5'-T G-3' 3'-ACC-5'	27.1	U2/5: 5'-G T-3' 3'-CCA-5'	27.3
M1/4: 5'- TG -3' 3'-AC-5'	39.1	M2/6: 5'-G T -3' 3'-CA-5'	39.8
U1/4: 5'-TG-3' 3'-AC-5'	41.5	U2/6: 5'-GT-3' 3'-CA-5'	40.2

T: DANP-anchored T.

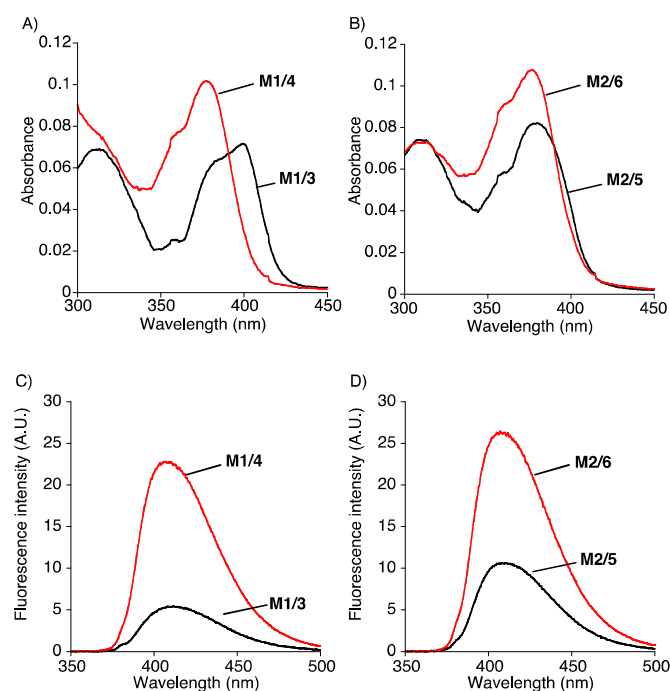


Fig. 2 A) and B) UV, and C) and D) fluorescence spectra of DANP-anchored DNA (4.5 μ M) in sodium phosphate buffer (pH 7.0, 10 mM) and sodium chloride (100 mM). Excitation wavelength was 380 nm. A) **M1/3** (black) and **M1/4** (red), B) **M2/5** (black) and **M2/6** (red), C) **M1/3** (black) and **M1/4** (red), D) **M2/5** (black) and **M2/6** (red).

The absorption maximum of the DANP-anchored duplexes was observed at 399 nm for **M1/3** holding the C-bulge and at 377 nm for the fully matched **M1/4** (Fig. 2A). The bathochromic shift by 22 nm suggested that the DANP anchored at the T in the 5'□**T**_G-3'/3'□ACC-5' bound to the flanking C-bulge. In contrast, only a slight bathochromic shift of the absorption peak was observed for the duplex **M2/5** as compared with **M2/6** (Fig. 2B), suggesting that the DANP anchored at the 5'□G_**T**-3'/3'□CCA-5' is not likely to bind to the C-bulge. These observations are in good agreement with the increase of T_m for

M1/3 not for **M2/5** The fully matched duplexes with anchored DANP (**M1/4** and **M2/6**) showed absorption maxima at 377 nm, regardless of the sequence, demonstrating that the anchored DANP was in a similar environment in both duplexes. As anticipated from the absorption spectra, the fluorescence change was more significant for the duplex containing **M1** than for the duplex containing **M2**. Thus, the fluorescence intensity increased by 4-fold due to the change from the C-bulge duplex **M1/3** to the fully matched duplex **M1/4** (Fig. 2C), whereas only a 2.5-fold increase was observed for the change from the C-bulge duplex **M2/5** to the fully matched duplex **M2/6** (Fig. 2D). This difference is due to the more pronounced fluorescence quenching in the 5'-T_{G-3'/3'-ACC-5'}, also suggesting that the DANP was bound to the C-bulge. The efficiency of quenching of DANP fluorescence anchored at the 5'-T_{G-3'/3'-AXC-5'} sequence, where the bulge base X is C, T, G, or A (Fig. S2), is roughly proportional to the efficiency of DANP binding we previously reported (C > T > G > A).³⁷

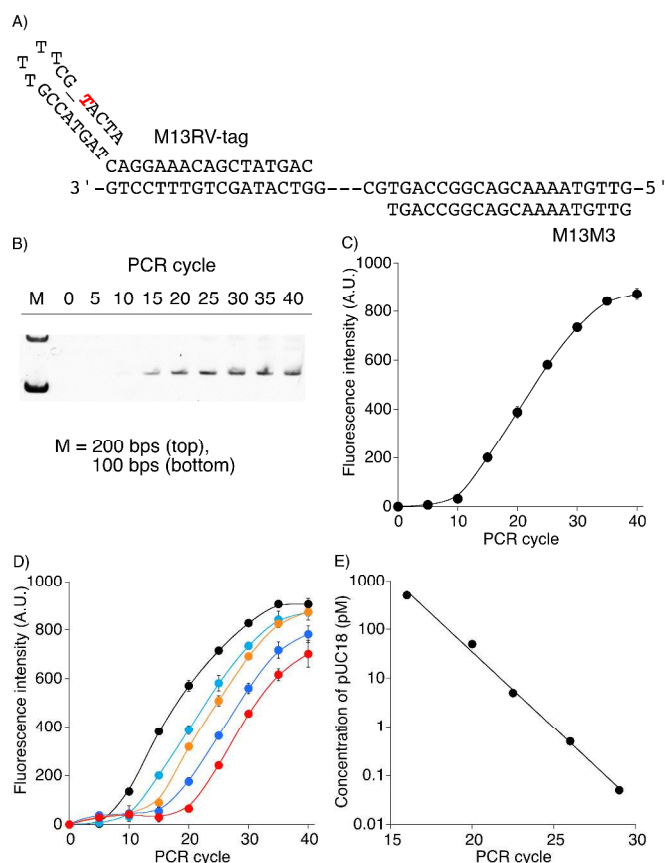


Fig. 3 Hairpin primer PCR with a DANP-anchored primer. A) Alignment of primers on the pUC18 template. Only one template strand is shown for clarity. B) PAGE analysis of PCR products. M: size marker, top: 200 bp, bottom: 100 bp. C) Fluorescence intensity of PCR solutions obtained from primers M13M3 and M13RV-tag using 50 pM concentrations of pUC18. The excitation wavelength was 355 nm. D) Fluorescence intensity of PCR solutions obtained with primers M13M3 and M13RV-tag under different concentrations of pUC18. Key: (black) 500 pM, (light blue) 50 pM, (orange) 5 pM, (blue) 0.5 pM, and (red) 0.05 pM. E) The standard plot obtained from Fig. 3D at 400 A.U. as a threshold cycle number. The vertical axis is the initial DNA concentration (logarithmic) and the horizontal axis is the PCR cycle number.

The 4-fold increase of DANP fluorescence observed by changing from the C-bulge form to the fully matched duplex encouraged us to

conduct quantitative PCR analysis with increasing fluorescent signals. The setup of PCR experiments using the DANP-anchored primer is illustrated in Fig. 3A. One of the PCR primers was labelled with a hairpin tag embedded to the C-bulge and the DANP-anchored T in the 5'-T_{G-3'/3'-ACC-5'} sequence (M13RV-tag). PCR was performed with the plasmid pUC18 as a template using the M13RV-tag primer and a non-labelled M13M3 primer. The PCR products were analysed using native polyacrylamide gel electrophoresis (PAGE) (Fig. 3B). The PCR product was obtained as a single band with a length of approximately 125 bp. Sequencing analysis of the PCR products revealed that adenine was incorporated opposite to the DANP-anchored T, indicating that the anchored DANP neither interfered with the DNA polymerase nor altered the nucleotide base to be incorporated during the polymerase reaction. The fluorescence intensity of the PCR solution started to increase after 10 PCR cycles under the conditions using 50 pM of the template, and reached a plateau after 35 cycles (Fig. 3C). The PCR product appeared on the PAGE gel at 15 cycles (cf. Fig. 3B), demonstrating consistency in the observations regarding the product formation by PAGE and fluorescence increase. With different template concentrations, the fluorescence intensity of the PCR solutions showed different threshold cycle numbers at a fluorescence intensity of 400 arbitrary units (A.U.) (Fig. 3D). An almost linear relationship was found between the logarithm of initial DNA concentrations and the PCR cycle number (Fig. 3E). These results clearly showed that hairpin primer PCR with the DANP-anchored primer could be used for quantitative real-time analysis of template concentration. In separate experiments, the results of DANP-anchored hairpin primer PCR were found to be consistent with those obtained with TaqMan[®] probes (Fig. S3). In addition, allele-specific PCR with the DANP-anchored hairpin primer clearly showed the discrimination of two alleles (Fig. S4).

In conclusion, DANP covalently anchored at the 5' T to the C-bulge in the 5'-T_{G-3'/3'-ACC-5'} stabilized the C-bulge and increased the fluorescence intensity induced upon structural changes from the C-bulge to the duplex by 4-fold. PCR with the hairpin primer containing DANP anchored to the T in the 5'-T_{G-3'/3'-ACC-5'} sequence successfully produced an increased fluorescence signal as the PCR cycle progressed. The linear correlation obtained between the logarithm of template concentration against PCR cycle number showed that the hairpin primer PCR with the DANP-anchored primer could be useful for real-time PCR.

This work was supported by Grant-in-Aid for Scientific Research (A) (23241073) for KN and (B) (24310165) for FT from the JSPS and by the Advanced research for medical products Mining Program of the National Institute of Biomedical Innovation (10-22) for KN. This research is partially supported by the Adaptable and Seamless Technology transfer Program through target driven R&D (A-STEP) from Japan Science and Technology Agency, JST for KN.

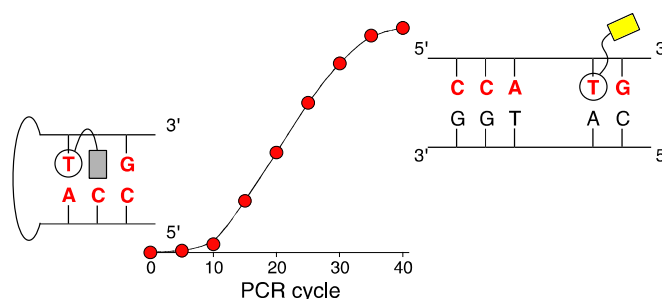
Notes and references

The Institute of Scientific and Industrial Research, Osaka University
8-1 Mihogaoka, Ibaraki, 567-0047 Japan,
E-mail: nakatani@sanken.osaka-u.ac.jp
Electronic Supplementary Information (ESI) available: [sequence of oligonucleotides, synthetic scheme, UV and Fluorescence spectra, and PCR experiments]. See DOI: 10.1039/c000000x/

- 1 S. Tyagi and F. R. Kramer, *Nat. Biotechnol.*, 1996, **14**, 303-308.
- 2 O. Köhler, D. V. Jarikote and O. Seitz, *ChemBioChem*, 2005, **6**, 69-77.

- 3 E. Socher, A. Knoll and O. Seitz, *Org. Biomol. Chem.*, 2012, **10**, 7363-7371.
- 4 F. Hövelmann, I. Gaspar, A. Ephrussi and O. Seitz, *J. Am. Chem. Soc.*, 2013, **135**, 19025-19032.
- 5 C. Holzhauser and H.-A. Wagenknecht, *Angew. Chem. Int. Ed.*, 2011, **50**, 7268-7272.
- 6 C. Holzhauser, R. Libel, A. Goepferich, H.-A. Wagenknecht and M. Breuning, *ACS Chem. Biol.*, 2013, **8**, 890-894.
- 7 M. A. Rubner, C. Holzhauser, P. R. Bohländer and H.-A. Wagenknecht, *Chem.-Eur. J.*, 2012, **18**, 1299-1302.
- 8 A. Okamoto, Y. Saito and I. Saito, *J. Photochem. Photobiol., C*, 2005, **6**, 108-122.
- 9 A. Okamoto, *Chem. Soc. Rev.*, 2011, **40**, 5815-5828.
- 10 Y. Xie, A. V. Dix and Y. Tor, *J. Am. Chem. Soc.*, 2009, **131**, 17605-17614.
- 11 R. W. Sinkeldam, N. Greco and Y. Tor, *Chem. Rev.*, 2010, **110**, 2579-2619.
- 12 M. S. Noe, A. C. Rios and Y. Tor, *Org. Lett.*, 2012, **14**, 3150-3153.
- 13 N. Venkatesan, Y. J. Seo and B. H. Kim, *Chem. Soc. Rev.*, 2008, **37**, 648-663.
- 14 A. P. Silverman and E. T. Kool, *Trends Biotechnol.* 2005, **23**, 225-230.
- 15 R. Häner, S. M. Biner, S. M. Langenegger, T. Meng and V. L. Malinovskii, *Angew. Chem. Int. Ed.*, 2010, **49**, 1227-1230.
- 16 S. G. Li, S. M. Langenegger and R. Häner, *Chem. Commun.*, 2013, **49**, 5835-5837.
- 17 H. Asanuma, M. Akahane, N. Kondo, T. Osawa, T. Kato and H. Kashida, *Chem. Sci.*, 2012, **3**, 3165-3169.
- 18 U. Englisch and D. H. Gauss, *Angew. Chem. Int. Ed. Engl.*, 1991, **30**, 613-629.
- 19 J. Guo, J. Y. Ju and N. J. Turro, *Anal. Bioanal. Chem.*, 2012, **402**, 3115-3125.
- 20 B. Juskowiak, *Anal. Bioanal. Chem.*, 2011, **399**, 3157-3176.
- 21 R. Amann and B. M. Fuchs, *Nat. Rev. Microbiol.*, 2008, **6**, 339-348.
- 22 K. Nakatani, *ChemBioChem*, 2004, **5**, 1623-1633.
- 23 A. C. Syvanen, *Nat. Rev. Genet.*, 2001, **2**, 930-942.
- 24 M. Strerath and A. Marx, *Angew. Chem. Int. Ed.*, 2005, **44**, 7842-7849.
- 25 G. Bao, W. J. Rhee and A. Tsourkas, *Annu. Rev. Biomed. Eng.*, 2009, **11**, 25-47.
- 26 P. M. Holland, R. D. Abramson, R. Watson and D. H. Gelfand, *Proc. Natl. Acad. Sci., U.S.A.*, 1991, **88**, 7276-7280.
- 27 C. A. Heid, J. Stevens, K. J. Livak and P. M. Williams, *Genome Res.*, 1996, **6**, 986-994.
- 28 H. A. Erlich, D. Gelfand and J. J. Sninsky, *Science*, 1991, **252**, 1643-1651.
- 29 M. V. Myakishev, Y. Khripin, S. Hu and D. H. Hamer, *Genome Res.*, 2001, **11**, 163-169.
- 30 A. C. Papp, J. K. Pinsonneault, G. Cooke and W. Sadee, *Biotechniques*, 2003, **34**, 1068-1072.
- 31 F. Takei, M. Igarashi, M. Hagihara, Y. Oka, Y. Soya and K. Nakatani, *Angew. Chem. Int. Ed.*, 2009, **48**, 7822-7824.
- 32 F. Takei and K. Nakatani, *Israel. J. Chem.*, 2013, **53**, 401-416.
- 33 T. Peng, H. He, M. Hagihara and K. Nakatani, *ChemBioChem*, 2008, **9**, 1893-1897.
- 34 F. Takei, M. Igarashi, Y. Oka, Y. Koga and K. Nakatani, *ChemBioChem*, 2012, **13**, 1409-1412.
- 35 H. Chen, F. Takei, E. S.-C. Koay, K. Nakatani and J. J. H. Chu, *J. Mol. Diagn.*, 2013, **15**, 227-233.
- 36 F. Takei, H. Tani, Y. Matsuura and K. Nakatani, *Bioorg. Med. Chem. Lett.*, 2014, **24**, 394-396.
- 37 H. Suda, A. Kobori, J. H. Zhang, G. Hayashi and K. Nakatani, *Bioorg. Med. Chem.*, 2005, **13**, 4507-4512.
- 38 F. Takei, H. Suda, M. Hagihara, J. H. Zhang, A. Kobori and K. Nakatani, *Chem.-Eur. J.*, 2007, **13**, 4452-4457.

A Table of Contents Entry



PCR progress could be monitored by increasing fluorescence using ligand-anchored hairpin primer.